Development 139, 1498-1508 (2012) doi:10.1242/dev.070367

Separating planar cell polarity and Hippo pathway activities of the protocadherins Fat and Dachsous

Hitoshi Matakatsu and Seth S. Blair*

SUMMARY

The giant *Drosophila* protocadherin Fat (Ft) affects planar cell polarity (PCP). Ft also inhibits the overgrowth of imaginal discs via the Hippo pathway, repressing the activity of the transcription co-factor Yorkie (Yki). Much of Ft activity is likely to be mediated by its intracellular domain (Ft ICD). However, the links between the Ft ICD and either PCP or Hippo activity are poorly understood, and the role of the Hippo pathway in PCP is ambiguous. We have performed a structure-function analysis of the Ft ICD. We found that the effects of the Ft ICD on PCP and the Hippo pathway are largely separable. Surprisingly, the domains required for PCP and Hippo activities do not map to any of the previously identified protein interaction domains, nor, with one exception, to the regions that are highly conserved in mammalian Fat4. We also found that the extracellular domain of Ft can act independently of the Ft ICD in PCP and can trigger dominant-negative and boundary effects on Hippo activity, probably via binding to the protocadherin Dachsous.

KEY WORDS: Fat, Fat4, Fat-J, Dachsous, PCP, Hippo, Warts, Lats, Yorkie, Expanded, Bantam

INTRODUCTION

The giant *Drosophila* protocadherin Fat (Ft) is required for the normal planar cell polarity (PCP) of several *Drosophila* tissues, including the orientation of hairs of the wing and abdomen and of larval denticles, and the orientation of fate choices in developing ommatidia (Casal et al., 2002; Rawls et al., 2002; Strutt and Strutt, 2002; Yang et al., 2002; Ma et al., 2003; Hogan et al., 2011; Donoughe and DiNardo, 2011), in a manner that in some contexts may be partly or wholly independent of the 'core' PCP pathway (Casal et al., 2006; Repiso et al., 2010; Donoughe and DiNardo, 2011). *ft* is also a known tumor suppresser gene that inhibits the overgrowth of imaginal discs (Bryant et al., 1988; Clark et al., 1995; Buratovich and Bryant, 1997; Garoia et al., 2000; Matakatsu and Blair, 2004). Ft activates the Hippo pathway, a group of interacting kinases and scaffolding proteins that normally repress the growth-inducing activity of the transcription co-factor Yorkie (Yki), which in turn regulates the transcription of target genes involved in cell proliferation and apoptosis (Bennett and Harvey, 2006; Cho et al., 2006; Silva et al., 2006; Willecke et al., 2006; Tyler and Baker, 2007; Oh and Irvine, 2008; Saucedo and Edgar, 2007; Pan, 2010). Removing Ft also leads to abnormal proximodistal patterning, causing joint loss in legs and the misplacement of crossveins in wings.

Ft binds in a preferentially heterophilic fashion to another large protocadherin, Dachsous (Ds) (Strutt and Strutt, 2002; Ma et al., 2003; Matakatsu and Blair, 2004). Preferentially heterophilic binding has also been observed between the mammalian homologs Fat4 (also known as Fat-J) and Dachsous 1 (Ishiuchi et al., 2009). Whereas Ft is uniformly expressed, Ds is expressed in patterns or gradients along the axes of many developing tissues. Ft-Ds binding is regulated further by phosphorylation of Ft and Ds cadherin repeats by the Golgi-resident kinase Four-jointed (Fj) (Ishikawa et al., 2008; Brittle et al., 2010; Simon et al., 2010), expression of which is often complementary to Ds expression. Patterned Ds binding is thought to modulate Ft activity, acting as a cue both for the orientation of PCP and for imaginal disc growth; indeed, experimentally altered gradients or boundaries of Fj, Ds or Ds extracellular domain (ECD) expression can reorient PCP (Adler et al., 1998; Zeidler et al., 1999; Zeidler et al., 2000; Strutt and Strutt, 2002; Yang et al., 2002; Ma et al., 2003; Matakatsu and Blair, 2004; Matakatsu and Blair, 2006) and trigger overgrowth by reducing Hippo pathway activity (Rogulja et al., 2008; Willecke et al., 2008). However, both pathways are also sensitive to unpatterned Ft-Ds binding, and some aspects of Ft activity are independent of Ds: PCP is largely normal in wings with uniform Ds and Fj expression, and loss of Ds and Fj causes only minor defects in wing growth (Matakatsu and Blair, 2004; Simon, 2004; Brittle et al., 2010).

Much of Ft activity is apparently mediated by the intracellular domain (ICD) of Ft (the Ft ICD), as expression of a version of Ft largely lacking its ECD rescues *ft* mutant overgrowth and greatly improves *ft* mutant PCP defects in the wing and abdomen (Matakatsu and Blair, 2006). However, the links between the Ft ICD and PCP or Hippo activity are poorly understood. The ICD of mammalian Fat4 has regions with substantial similarity to *Drosophila* Ft (Fig. 1; supplementary material Fig. S1) (Hong et al., 2004), which is suggestive because loss of Fat4 has been linked to PCP defects in vivo (Saburi et al., 2008), as has loss of its binding partner Dachsous 1 (Mao et al., 2011). Loss of Fat4 is tumorigenic in vitro (Qi et al., 2009) and increases the number of Hippo-regulated neuronal precursors in chicks (Van Hateren et al., 2011).

A few binding partners for the Ft ICD have been identified. Lowfat binds Ft, Fat4 and Ds and plays a weak modulatory role, increasing the levels of Ft and Ds at the cell membrane (Mao et al., 2009). The transcriptional co-regulator Atrophin/Grunge binds the C-terminal region of the Ft ICD and might play a role

Department of Zoology, University of Wisconsin-Madison, 250 North Mills Street, Madison, WI 53706, USA.

*Author for correspondence (ssblair@wisc.edu)

Accepted 17 February 2012

+ = strong, +/- = weak -/+ = very weak - = undetectable		Rescues *ft* abdominal PCP (*actin-gal4*)		Rescues *ft* eclosion (*actin-gal4*)		Rescues *ft* *ex-lacZ* &/or *ban3-GFP* (*hh-gal4*)		Rescues *ft* overgrowth (*hh-gal4*)		Up-regulation of *ex-lacZ* &/or *ban3-GFP* in wild type (*hh-gal4*)
Short name	**Deletion from ICD**	**ΔECD**	**+ECD**	**ΔECD**	**+ECD**	**ΔECD**	**+ECD**	**ΔECD**	**+ECD**	**+ECD**
FtΔECD or Ft		+	+	+	+	+	+	+	+	bound.
ΔN-1	4614-4701	-/+	+/-	+	+	+	+	+	+	bound.
ΔN-2	4614-4733	-/+	+/-	+	+	+	+	+	+	bound.
ΔN-4	4614-4774	-	-/+	+	+/-	+/-	+/-	+/-	+/-	bound.
ΔN-5	4614-4836	-	-/+	-	-	-	-	-	-	bound.+ post.
ΔN-6	4614-4914	-	-/+	-	-	-	-	-	-	bound.+ post.
Δ9-C	5122-5147	+	+	+	+	+	+	+	+	bound.
Δ8-C	5084-5147	+	+	+	+/-	+	+/-	+	+/-	bound.
Δ7-C	5035-5147	+	+	+	+	+	-	+	+/-	bound.+ post.
Δ6-C	4921-5147	+	+	+	-	+	+/-	+	+	bound.+ post.
Δ5-C	4839-5147	+	+	-	-	-	-	-	-	bound.+ post.
ΔICD	4620-5147	-	-/+	-	-	-	-	-	-	bound.+ post.
Δ4-C	4784-5147	+		-		-		-		
Δ2-C	4734-5147	+		-		-		-		
Δ1-C	4707-5147	+		-		-		-		
Δ5-6	4840-4920	+		-		-/+		-		
Δ1-3	4701-4752	+		+		+		+		
Δ3-4	4753-4774	+		+		+		+		
Δ3-5	4753-4836	+		-		-/+		-		
Δ1-5	4701-4836	+		-		-/+		-		

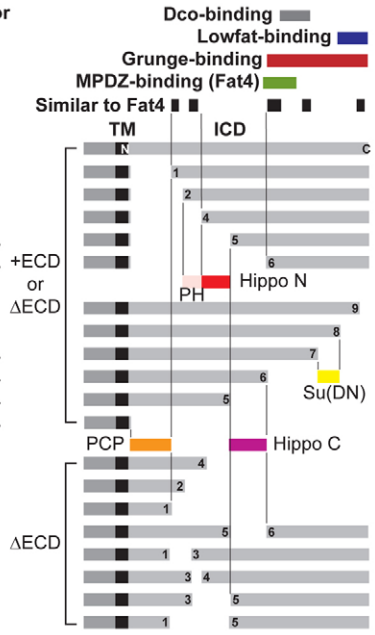

Fig. 1. Summary of constructs and their ability to rescue *ft* mutant phenotypes or induce dominant-negative phenotypes in wild-type *Drosophila*. The short names of the constructs are shown in the first column and the positions of the deleted amino acids in the second. The rescue of *ft* PCP defects in the dorsolateral regions of anterior abdomens was tested using *actin-gal4*-driven expression of constructs lacking (ΔECD) or containing (+ECD) the ECD of Ft (see Fig. 3; supplementary material Fig. S3; Table 1). For rescue of eclosion in *ft* by *actin-gal4*-driven construct expression, + indicates 10% of wild-type eclosion, +/– indicates 1-10% and – indicates 0% (supplementary material Fig. S5). For rescue of heightened *ex-lacZ* and/or *ban3-GFP* expression in *ft* wing discs by *hh-gal4*-driven construct expression, + indicates robust downregulation in dorsal and ventral hinge, +/– indicates weak dorsal but stronger ventral, –/+ indicates very weak dorsal and weak ventral and – indicates not detectable (Fig. 4; supplementary material Figs S6-S8). Quantification of rescue of *ft* wing disc overgrowth by *hh-gal4*-driven construct expression is shown in supplementary material Fig. S9. The upregulation of *ex-lacZ* and/or *ban3-GFP* expression in wild-type wing discs caused by posterior, *hh-gal4* expression of +ECD constructs was scored as being limited to the boundary of overexpression (bound.), or in boundary and posterior cells (bound. + post.) (Fig. 5; supplementary material Fig. S10; see supplementary material Fig. S11 for data on the effects on growth). The map shows the deduced positions of the PCP, PH, Hippo C, Hippo N and Su(DN) regions based on these data. Known features of and binding sites for the Ft ICD are shown at the top right. See supplementary material Fig. S1 for more detailed mapping of deduced regions to the amino acid sequences of Ft and Fat4.

in PCP (Fanto et al., 2003). Mammalian Fat4 binds the PDZ-containing scaffolding protein Mpdz (also known as Mupp1) and its binding partner Pals1 (Mpp5 – Mouse Genome Informatics), and loss of any of these disrupts adhesion between cortical cells apical to the adherens junctions (Ishiuchi et al., 2009). This could also provide a link to PCP, as loss of *Drosophila* Mpdz/Patj has subtle effects on eye PCP (Djiane et al., 2005). The casein kinase Discs overgrown (Dco) binds to and phosphorylates the Ft ICD, and loss of Dco causes imaginal disc overgrowth (Feng and Irvine, 2009; Sopko et al., 2009). However, there have been no experiments published that test the importance of these binding sites, and the domains that are critical for the activity of the Ft ICD have not been identified.

There has also been debate about the number of genetic and biochemical pathways downstream of the Ft ICD. Some mutants that act genetically downstream of *ft* appear to be more important in Hippo signaling and affect PCP and limb patterning more weakly, such as those affecting the atypical myosin Dachs, its regulator Approximated, and the FERM scaffolding protein Expanded (Mao et al., 2006; Feng and Irvine, 2007; Matakatsu and Blair, 2008). Unpatterned increases in Hippo activity can rescue *ft* mutant overgrowth without greatly improving PCP or appendage-patterning defects (Feng and Irvine, 2007). However, as the biochemical links to the Ft ICD are not known it is not clear at what level the PCP and Hippo pathways diverge. And because the Hippo pathway also regulates the expression of *fj*, overlap between Hippo and PCP activities has also been hypothesized (Feng and Irvine, 2007).

We have therefore taken a structure-function approach to identify the domains of the Ft ICD that are crucial for PCP and Hippo pathway activity, and to see whether we can identify pathway-specific domains. We will show that such pathway-specific domains can be found. Notably, these domains do not correspond to previously reported protein-binding domains, nor, with one exception, the regions most similar to the ICD of Fat4.

We have also examined the activity of the ECD of Ft. We show that it retains slight activity in PCP, consistent with other data suggesting that Ft can influence PCP by signaling through Ds (Casal et al., 2006). The ECD of Ft can also exert 'dominant-negative' effects on Hippo activity in neighboring cells (Zecca and Struhl, 2010), and this effect can be increased by removal of the Ft ICD (Matakatsu and Blair, 2006; Willecke et al., 2006). We identify domains within the ICD that contribute to this effect, and present evidence that it is partially mediated by the Ds in adjacent cells, and can be reproduced by the ICD of Ds. This extends recent evidence that Ds acts not only as a ligand for Ft, but also as a

receptor for Ft, and that both can have positive and negative effects on Hippo pathway activity (Willecke et al., 2006; Zecca and Struhl, 2010).

MATERIALS AND METHODS

Ft constructs and transformant lines

Ft and Ds extracellular and intracellular deletion constructs were previously described (Matakatsu and Blair, 2004; Matakatsu and Blair, 2006). New *UAS-"ftX"* constructs were inserted between *Not*I site and *Kpn*I sites in pUAST. The protein sequences are listed in supplementary material Table S1. FtΔX constructs were HA-tagged at their C-termini, except for FtΔ5-C and FtΔECDΔ5-C. Anti-HA or anti-Ft staining was used to confirm comparable expression levels in vivo.

ban3-GFP, derived from the *Sal*I-*Eco*RV fragment of the regulatory region of *bantam* (Tanaka-Matakatsu et al., 2009), was cloned between the *Nae*I and *Xho*I sites of pH-stinger (Barolo et al., 2000).

Drosophila stocks and crosses

We used the following crosses: Rescue of eclosion and abdominal hair polarity in *ft* mutants: usually $ft^{G\text{-}rv}$; *actin-gal4 / CyO-TM6,Tb* to ft^{fd}; *UAS-ftX / CyO-TM6,Tb*; in a few cases we used instead *UAS-ftX* insertions on the second or first chromosome. Rescue of PCP in *ds ft* double mutants: ds^{UAO71} $ft^{G\text{-}rv}$; *actin-gal4/CyO-TM6,Tb to* ds^{UAO71} ft^{fd}; *UAS-ftX/CyO-TM6,Tb*. *ex-lacZ* in *ft* mutants: ft^{spy} *ex-lacZ/+*; *hh-gal4 UAS-GFP/+* males to ft^{fd}; *UAS-ftX/CyO-TM6,Tb* females, and checking offspring discs for the presence of *ex-lacZ* and *hh-gal4*-driven GFP. *ban3-GFP* in *ft* mutants: ft^{fd}; *hh-gal4 ban3-GFP/CyO-TM6,Tb* females to ft^{fd}; *UAS-ftX/CyO-TM6,Tb* males. *ex-lacZ* in wild-type discs: *ex-lacZ; hh-gal4/CyO-TM6,Tb* to *UAS-ftX*. The effects of *UAS-ft* overexpression on *ban3-GFP* in wild-type or *ds* mutant discs: ds^{UAO71} $ft^{G\text{-}rv}$; *hh-gal4 ban3-GFP/CyO-TM6,Tb* females to *UAS-ft/Y*; ds^{05142}/+ males, and checking female offspring discs for the presence or absence of anti-Ds staining or ds^{05142}-driven *lacZ* expression. *ban3-GFP* expression in the *ds*, *ft* and *ds ft* mutant discs: ds^{UAO71} $ft^{G\text{-}rv}$; *hh-gal4 ban3-GFP/CyO-TM6,Tb* to either ds^{UAO71}; *UAS-ftX/CyO-TM6,Tb* or ft^{fd}; *UAS-ftX / CyO-TM6,Tb* or ds^{UAO71} ft^{fd}; *UAS-ftX/CyO-TM6,Tb*. *ban3-GFP* expression in *fj* heterozygotes or homozygotes: fj^{d1}; *UAS-ft/TM6,Tb* stock to either fj^{d1}; *hh-gal4 ban3-GFP/TM6,Tb* or *hh-gal4 ban3-GFP/TM6,Tb* flies. *ft* and *wts* clones: *yw hs-FLP;* FRT^{40} *arm-lacZ; ban3-GFP/CyO-TM6,Tb* to ft^{fd} FRT^{40}*/CyO*, or *yw hs-FLP*; FRT^{82} *arm-lacZ/TM6,Tb* to *ban3-GFP/CyO;* wts^{X1} FRT^{82}*/TM6b,Tb*.

Quantification of abdominal hair polarity

Dissected abdomens were mounted in Hoyer's solution and the angles of all the hairs in the region from the dorsal to the lateral midline of each pigmented anterior compartment (supplementary material Fig. S3A, red outline) were measured using the line segment tool in Adobe Illustrator.

Immunohistochemistry

Antibody staining was performed according to Blair (Blair, 2000) with the following primary antibodies: rabbit anti-βgal (Cappell), mouse anti-βgal (Developmental Studies Hybridoma Bank), rat anti-Ci (Motzny and Holmgren, 1995), rabbit anti-HA (Santa Cruz Biotechnology), rat anti-HA (Roche), rabbit anti-Ds (Strutt and Strutt, 2002), rat anti-Ds and rat anti-Ft (Yang et al., 2002). Images were taken using a Biorad laser scanning confocal microscope.

RESULTS

Activity of the Ft ICD

Ubiquitous, *actin-gal4*-driven expression of a construct lacking most of the ECD of Ft (FtΔECD) in the *ft* null mutant combination $ft^{G\text{-}rv}/ft^{fd}$, rescues disc overgrowth, allows eclosion, and substantially improves hair PCP defects in wings (Fig. 2A-C; supplementary material Fig. S2A,B,D) and abdomens (supplementary material Fig. S3A,B,G; quantification of hair polarity in the anterior compartment of the abdomen is shown in Table 1) (Matakatsu and Blair, 2006). Although FtΔECD did not detectably bind Ds in vitro or stabilize Ds in vivo, it retains a portion of the first of the 34 cadherin domains of Ft. To rule out extracellular regulation by Ds or other ligands, we made a larger deletion that removes all of the cadherin domains (FtΔECD2). FtΔECD2 rescued imaginal disc overgrowth (supplementary material Fig. S7B, quantified in supplementary material Fig. S9) and eclosion (supplementary material Fig. S5) and improved PCP in *ft* mutant wings (Fig. 2D) and abdomens (Fig. 3A,B,D; supplementary material Fig. S3H; Table 1). We also tested whether the transmembrane domain of Ft was required for its activity by expressing a λFtICD protein consisting of an extracellular region largely derived from the cI dimerization domain of the λ repressor, a transmembrane domain from *Drosophila* Breathless (Lee et al., 1996; Queenan et al., 1997), and the ICD of Ft (amino acids 4611-5147). Although not as active as FtΔECD or FtΔECD2, λFtICD rescued imaginal disc overgrowth (supplementary material Fig. S7C, Fig. S9) and eclosion (supplementary material Fig. S5) and improved PCP in *ft* mutant wings (Fig. 2E) and abdomens (Fig. 3E; supplementary material Fig. S3I; Table 1). Therefore, neither the ECD nor the transmembrane domains of Ft is completely required for its function. By contrast, a construct containing just the ICD of Ft (FtICD; 4611-5147) did not rescue disc overgrowth (supplementary material Fig. S7D, Fig. S9) or eclosion (supplementary material Fig. S5) or detectably improve PCP defects in the abdomen (supplementary material Fig. S3J; Table 1).

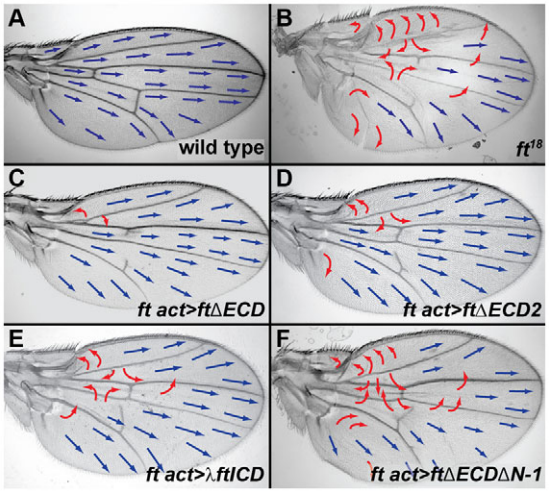

Fig. 2. Hair PCP in wings. Blue arrows indicate normal wing hair polarity, and red arrows abnormal polarity. (**A**) Normal polarity in wild-type *Drosophila*. (**B**) Abnormal polarity in viable, hypomorphic ft^{18} mutation. (**C-F**) Improvement of polarity in $ft^{G\text{-}rv}/ft^{fd}$ null mutant combination after *actin* (*act*)*-gal4*-driven expression of *UAS-ftΔECD* (C), *UAS-ftΔECD2* (D) or *UAS-λftICD* (E), but little improvement by *UAS-ftΔECDΔN-1* (F). See supplementary material Fig. S2 for results with additional FtΔECD and Ft+ECD constructs.

The PCP rescue achieved with uniform expression of FtΔECD, FtΔECD2 or λFtICD was not perfect, especially in the posterior of abdominal segments or in the proximal portion of the wing blade (Fig. 2C-E; supplementary material Fig. S2; Table 1) (Matakatsu and Blair, 2006). This is not surprising, as the activity of these constructs cannot be spatially regulated by binding the ECD of Ds, or by spatially restricted phosphorylation of the cadherin domains of Ft by Fj. That said, when we quantified hair polarity in the anterior compartment of the abdomen, rescue by *actin-gal4*-driven *UAS-ftΔECD* or *UAS-ftΔECD2* was similar to the rescue by *UAS-ft* (Table 1). *actin-gal4*-driven Ft or FtΔECD expression also

Table 1. Percentage of abdominal hairs with greater than 30° divergence from posterior orientation (*n*)

Wild type	*ft*	*ft act>ft*	*ft act> ftΔECD*	*ft act> ftΔECD2*	*ft act> λftICD*	*ft act> ftICD*	*ft act> ftΔECDΔ1-C*	*ft act> ftΔECDΔICD*	*ft act> ftΔECDΔN-1*	*ft act> ftΔECDΔN-4*	*ft act> ftΔN-1*	*ft act> ftΔICD*
1.5% (4517)	51.3% (11,963)	14.7% (4473)	18.6% (3523)	10.9% (1584)	27.4% (1872)	55.9% (3406)	22.4% (5590)	58.8% (2167)	38.8% (3523)	48.5% (4850)	26.9% (2907)	36.4% (3536)

Measured only in the region from the dorsal to the lateral midline of each pigmented anterior compartment (red outline in supplementary material Fig. S3A).

substantially improved wing and abdominal hair polarity in *ds* mutants (not shown) and *ds ft* double mutants (supplementary material Fig. S2M,N, Fig. S3P,Q). Rescue in the absence of the ECD of Ft or Ft-Ds binding suggests that the Ft ICD has a strong permissive role in PCP (see Discussion). *actin-gal4*-driven Ds overexpression did not detectably improve PCP in *ft* mutant abdomens (Fig. 3F).

PCP-active domains in the Ft ICD

We next generated deletions from FtΔECD that began either at the C terminus of its ICD (amino acid 5147 in wild-type Ft) or near the N-terminal end of its ICD (amino acid 4614 in wild-type Ft). In our terminology, N and C denote the termini of the ICD, and the numbers 1-9 indicate approximate break points between the termini; the exact breakpoints are shown in Fig. 1 and supplementary material S1A and Table S1. When expressed in wing discs, these deleted FtΔECD proteins localized to internal cellular structures and weakly to the cell membrane, much like FtΔECD (Matakatsu and Blair, 2006), but did not concentrate in the sub-apical cell membrane like full-length Ft (not shown). Not all of our deleted constructs rescued viability and wing disc overgrowth in *ft* mutants (see below), and the distortions in the overgrown wings prevented us from examining their wing hair polarity. *ft* mutant abdomens, however, do not overgrow, so we were able to compare hair polarity in different pharate (pre-eclosed) abdomens. For reasons of brevity, the data is summarized in Fig. 1, and the remaining figures show only the results with constructs that identify critical ICD domains.

We could remove large regions of the ICD without reducing the rescue of abdominal hair polarity (Fig. 1). Moreover, FtΔECDΔ1-C, which retains only 91 amino acids of the ICD near the transmembrane domain, rescued PCP almost as well as FtΔECD, whereas the larger deletion in FtΔECDΔICD did not detectably rescue (Fig. 3G,H; supplementary material Fig. S3M,N; Table 1). FtΔECDΔ1-C also improved PCP in *ds ft* double mutant abdomens (supplementary material Fig. S3S). Deleting the N-1 region also markedly reduced the rescue of *ft* mutant PCP defects in the abdomen (FtΔECDΔN-1; Fig. 3I; supplementary material Fig. S3K; Table 1), and reduced PCP rescue in the wing: wing hair polarity in *ft* null mutants expressing FtΔECDΔN-1 or FtΔECDΔN-2 was similar to that of the viable ft^{18} hypomorph (Fig. 2B,F; supplementary material Fig. S2H,J). Thus, we have identified a very small 'PCP' region of the Ft ICD (N-1, amino acids 4620-4701; orange in Fig. 1) that is necessary and sufficient for much of the PCP activity of the ICD.

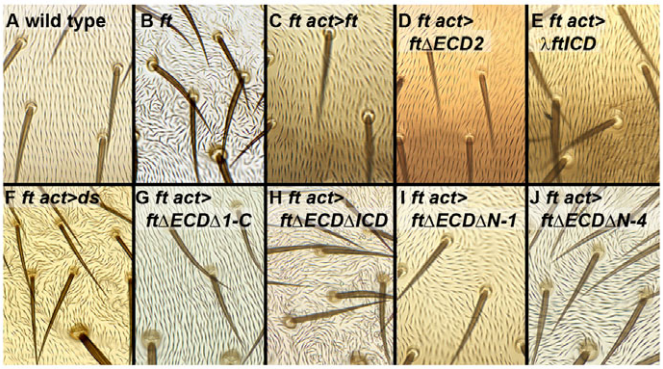

Fig. 3. Hair polarity in the anterior portions of pharate or adult abdominal segments. (**A**) Normal polarity in wild-type *Drosophila*. (**B**) Abnormal polarity in $ft^{G\text{-}rv}/ft^{fd}$. (**C-J**) Polarity in $ft^{G\text{-}rv}/ft^{fd}$ after *act-gal4*-driven expression of *UAS-ft* (C), *UAS-ftΔECD2* (D), *UAS-λftICD* (E), *UAS-ds* (F), *UAS-ftΔECDΔ1-C* (G), *UAS-ftΔECDΔICD* (H), *UAS-ftΔECDΔN-1* (I) or *UAS-ftΔECDΔN-4* (J). See supplementary material Fig. S3 for results with additional FtΔECD and Ft+ECD constructs, and Table 1 for quantification.

However, FtΔECDΔN-1 and FtΔECDΔN-2 still showed very weak improvement of *ft* mutant PCP in the abdomen, suggesting the involvement of other regions of the ICD. FtΔECDΔN-4, by contrast, did not detectably improve *ft* mutant PCP (Table 1; Fig. 3J; supplementary material Fig. S3L). This identifies a region between positions 2 and 4 that is weakly active in abdominal PCP (amino acids 4734-4774; pink in Fig. 1). We will show below that this region also plays a weak role in Hippo activity, so we termed this region PH for PCP-Hippo.

Hippo-active domains of the Ft ICD

Next, we investigated whether the regulation of viability, growth and the Hippo pathway by FtΔECD relied upon the same regions as those active in PCP. We used *actin-gal4* to test rescue of eclosion. To assess directly the effects on the Hippo pathway, we examined expression of the Yki target gene *expanded* (*ex*) using the *ex-lacZ* enhancer trap (Boedigheimer and Laughon, 1993). *ex-lacZ* expression is upregulated in *ex-lacZ ft/ft* wing discs (Willecke et al., 2006), and in our hands provides a more sensitive marker than Thread (also known as Diap1), Cyclin E or *fj-lacZ*. We also replicated several experiments using *ban3-GFP*, a reporter derived from the regulatory region of the *bantam* (*ban*) miRNA (Tanaka-Matakatsu et al., 2009). Like sensors for the *ban* miRNA (Nolo et al., 2006; Thompson and Cohen, 2006), *ban3-GFP* responds to changes in Ft and Hippo activity (supplementary material Fig. S4A,B), and has a sensitivity similar to that of *ex-lacZ*.

To provide an internal control, we limited Ft construct expression to the posterior compartment of *ft* mutant wing discs using *hh-gal4*, identifying the region of expression with either *UAS-GFP*, or C-terminal HA tags on the constructs (Fig. 4; supplementary material Figs S6-S8). Posterior, *hh-gal4*-driven expression of *UAS-ftΔECD* or *UAS-ftΔECD2* in *ft* mutant wing discs reduced posterior overgrowth (quantified in supplementary material Fig. S9) and cell-autonomously reduced *ex-lacZ* and *ban3-GFP* expression; the effect on *ex-lacZ* and *ban3-GFP* was especially strong in the prospective dorsal and ventral hinge regions of the wing disc (supplementary material Fig. S7B).

The effects that our constructs had on eclosion, the expression of *ex-lacZ* and *ban3-GFP* or on overgrowth in *ft* mutant discs, were largely congruent, as summarized in Fig. 1 (the other main figures show only constructs that identify critical domains; more

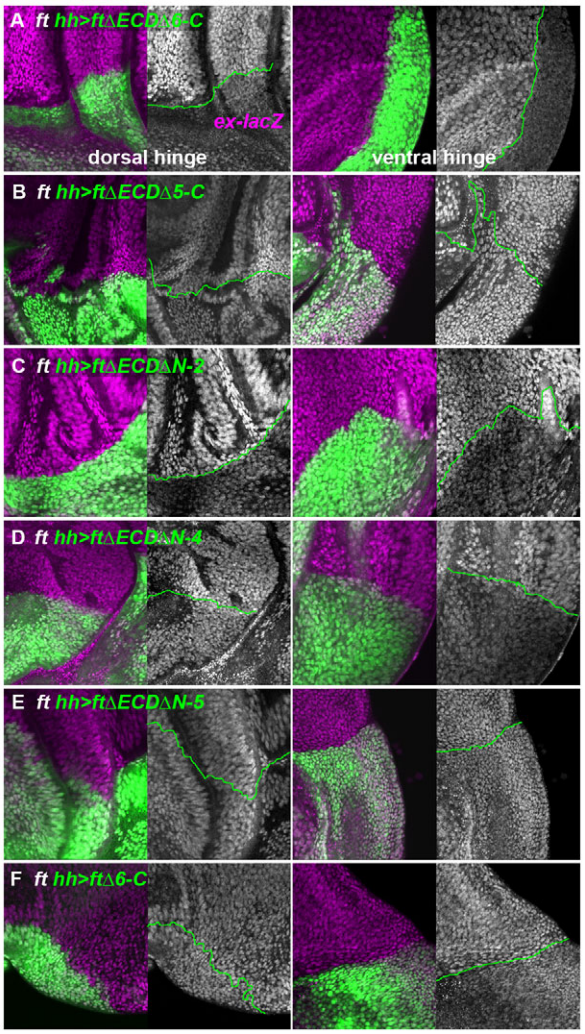

Fig. 4. Ability of *hh-gal4*-driven expression of *UAS-ft* constructs to reduce heightened *ex-lacZ* expression in ft^{spy} *ex-lacZ*/ft^{fd} mutant wing discs. (**A-F**) Frames show details of expression in the prospective dorsal and ventral hinge regions of the disc. The domains of *hh-gal4* expression were identified with *UAS-GFP* (green, boundaries outlined in green in *ex-lacZ*-only frames). Expression of *ex-lacZ* (purple or white) is reduced by *UAS-ftΔECDΔ6-C* (A), *UAS- ftΔECDΔN-2* (C), *UAS-ftΔECDΔN-4* (D) or *UAS-ftΔ6-C* (F), but is not reduced by *UAS-ftΔECDΔ5-C* (B) or *UAS- ftΔECDΔN-5* (E). See supplementary material Fig. S6 for *ex-lacZ* results with additional FtΔECD constructs and lower magnification photos, and supplementary material Fig. S7 for *ft* rescue experiments with the *ban3-GFP* marker.

comprehensive figures, including those showing overgrowth, are in supplementary material Figs S6-S8, and quantification of growth effects are shown in supplementary material Fig. S9). Large portions of the ICD of FtΔECD could be removed, including the PCP region, without blocking or obviously reducing its rescuing activity (e.g. FtΔECDΔ6-C, Fig. 4A; FtΔECDΔN-2, Fig. 4C). However, larger deletions (e.g. FtΔECDΔ5-C or FtΔECDΔN-5) did not detectably rescue eclosion (Fig. 1; supplementary material Fig. S5) or reduce heightened *ex-lacZ* or *ban3-GFP* expression or overgrowth (Fig. 4B,E; supplementary material Fig. S6D,I, Fig. S7G,M, Fig. S9). These results define two adjacent central regions of the ICD that we termed Hippo N (4-5, amino acids 4775-4836; red in Fig. 1) and Hippo C (5-6, amino acids 4839-4920; purple in Fig. 1). FtΔECDΔN-4 rescued eclosion (supplementary material Fig. S5) and reliably reduced heightened *ex-lacZ* expression in the ventral hinge of the wing disc, but poorly reduced heightened *ex-lacZ* in the dorsal hinge region of the wing disc (Fig. 4D), indicating that the PH region (2-4, amino acids 4734-4774, pink in Fig. 1) also has a weak role in Hippo pathway activity.

Smaller internal deletions of the ICD confirmed the importance of Hippo N and Hippo C. Constructs lacking Hippo N (4-5) and part of PH (2-4) (FtΔECDΔ3-5), or lacking Hippo C (5-6) (FtΔECDΔ5-6), did not rescue eclosion (supplementary material Fig. S5) or overgrowth (supplementary material Fig. S9), and only very weakly reduced heightened *ex-lacZ* (supplementary material Fig. S8A,B); FtΔECDΔ5-6 was slightly more effective reducing *ex-lacZ* than FtΔECDΔ5-C. Constructs lacking complementary portions of PH (2-4) (FtΔECDΔ1-3 or FtΔECDΔ3-4) rescued eclosion (supplementary material Fig. S5) and overgrowth (supplementary material Fig. S9) and strongly reduced heightened *ex-lacZ* (supplementary material Fig. S8C,D), consistent with a weaker role for the PH region.

A surprising feature of our results is that much of the Ft ICD, including known protein-binding domains, are disposable for its Hippo and PCP activities (Fig. 1; see Discussion). As our assays were also performed using constructs lacking most of the ECD of Ft, one possibility is that these disposable regions might play a role in the spatial regulation of Ft activity after Ds binding to and Fj phosphorylation of the ECD. We therefore also tested the activity of constructs containing the ECD of Ft ('Ft+ECD') but similarly lacking portions of the ICD. However, these results were more difficult to interpret because of two factors: first, an ICD-independent effect of Ft on PCP, and second, a dominant-negative effect on Hippo activity caused by the ECD of Ft.

An ICD-independent PCP activity for the ECD of Ft

When expressed in wing discs, Ft+ECD proteins concentrated in the sub-apical cell membrane (not shown). Although the effects of these constructs were largely congruent with the effects of our FtΔECD constructs (Fig. 1), many of our Ft+ECD constructs did a slightly better job rescuing hair polarity in *ft* mutant abdomens and wings than their ΔECD counterparts. For instance, Ft+ECD constructs that lacked the PCP region of the ICD nonetheless slightly improved PCP in *ft* mutant abdomens and wings (e.g. ΔN-1: supplementary material Fig. S2G,H, Fig. S3E,K; Table 1). This is consistent with the hypothesis that some of the ICD regions outside of the PCP region, which are disposable for the PCP activity of ΔECD constructs, can play a more important role in the presence of the ECD, and, thus, in the presence of spatially regulated Ft-Ds binding, or when the proteins are concentrated at the sub-apical cell membrane.

However, FtΔICD, which lacks all but five amino acids of the ICD; could also weakly improve PCP in *ft* mutant abdomens (Table 1), indicating that the ECD of Ft has a weak PCP activity that does not rely on the Ft ICD. This makes it difficult to attribute with any certainty the improvement of PCP activity in +ECD constructs to improved activity of the Ft ICD. Because FtΔICD can bind Ds (Matakatsu and Blair, 2006), it is likely that Ft-bound Ds carries redundant PCP activity in the absence of the Ft ICD. Indeed, although FtΔN-1 improved PCP in *ft* mutant abdomens, it did not noticeably improve PCP in *ds ft* double mutant abdomens (supplementary material Fig. S3R). As Ft can rescue abdominal PCP in a *ds ft* double mutant, the lack of rescue with FtΔN-1 shows that the PCP region (N-1) is necessary for rescuing *ds ft* abdominal PCP, even in constructs containing the ECD of Ft (supplementary

material Fig. S3O,P,R). The PCP region is also sufficient, as the *ds ft* PCP phenotype was improved by FtΔECDΔ1-C (supplementary material Fig. S3S).

Portions of the ICD suppress a dominant-negative Hippo activity of the ECD of Ft

Testing the abilities of Ft+ECD constructs to rescue eclosion and Hippo activity in *ft* mutants confirmed the importance of the PH, Hippo N and Hippo C domains (Fig. 1). However, in some cases the Ft+ECD constructs did a worse job rescuing the lethality and heightened *ex-lacZ* or *ban3-GFP* expression of *ft* mutants than their FtΔECD counterparts. This is likely to be due to an unusual effect of the ECD of Ft: its ability to induce dominant-negative, *ft* mutant-like effects on the Hippo pathway.

Misexpressing a version of Ft lacking the ICD (FtΔICD) has a dominant-negative effect on Hippo pathway activity, inducing overgrowth in wild-type discs (Matakatsu and Blair, 2006) and heightening the expression of *ex-lacZ* (Willecke et al., 2006) (Fig. 5A) or *ban-3-GFP* (see below) throughout the region of misexpression. The effects of posterior *hh-gal4*-driven *UAS-ftΔICD* expression on growth and reporter gene expression were especially strong in the prospective hinge regions of the wing disc, and extended into neighboring cells in the anterior compartment.

Deletion of particular regions of the ICD from +ECD constructs also caused dominant-negative effects on growth and Hippo pathway activity that were similar to those caused by FtΔICD in wild-type discs (Fig. 5; supplementary material Figs S10, S11; 'posterior + bound.' in Fig. 1). *hh-gal4*-driven FtΔ7-C expression caused posterior and boundary dominant-negative effects, whereas the smaller deletion in FtΔ8-C largely blocked the posterior effect, retaining only the boundary effect (Fig. 5B,C); we discuss the boundary effect in more detail below. This identifies a region between positions 7 and 8 (amino acids 5035-5084) that is required to suppress the dominant-negative effects of the ECD [we term this region Su(DN); yellow in Fig. 1]. Because the Su(DN) region is not required for Hippo activity in FtΔECD constructs, and as the effect of removing it from Ft+ECD is non-autonomous (Fig. 5B), the effect is likely to be mediated by changing the activity of the ECD of Ft. However, the effect was not accompanied by any detectable difference in the levels or localization of the construct proteins.

Su(DN) is not, however, the only region that suppresses the dominant-negative effects of posterior Ft overexpression. FtΔ5-C, which lacks both Su(DN) (7-8) and Hippo C (5-6), or the smaller deletion in FtΔ6-C, both caused slightly stronger overgrowth than the removal of Su(DN) with FtΔ7-C (supplementary material Fig. S10B-E; overgrowth quantified in supplementary material Fig. S11). FtΔN-5, which lacks Hippo N but not Su(DN), also induced much stronger overgrowth and 'posterior + boundary' upregulation of Yki targets (Fig. 5D; supplementary material Fig. S10J, Fig. S11G), whereas FtΔN-4, which leaves Hippo N intact, induced weaker overgrowth and only slightly increased Yki targets in the posterior (Fig. 5E; supplementary material Fig. S10I, Fig. S11F). This suggests that regions outside of Su(DN), including Hippo N and Hippo C, can alter the activity of the ECD of Ft.

FtΔICD expression can increase overgrowth (supplementary material Fig. S9) (Matakatsu and Blair, 2006) and slightly increase *ex-lacZ* or *ban3-GFP* in *ft* mutant discs (Fig. 5F; supplementary material Fig. S12A,B). Therefore, ECD-induced dominant-negative effects might be expected to negatively impact the rescue of *ft* mutants. Indeed, *hh-gal4*-driven FtΔECDΔ6-C and FtΔECDΔ7-C strongly rescued overgrowth and suppressed *ex-lacZ* expression in

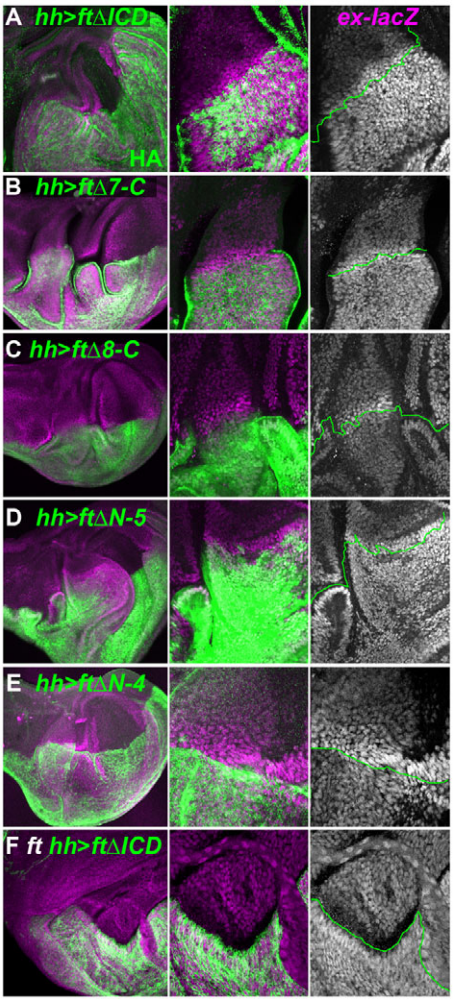

Fig. 5. Reaction of *ex-lacZ* expression to *hh-gal4*-driven posterior expression of *UAS-ft* constructs in wild-type and *ft* mutant wing discs. *ex-lacZ* expression is in purple or white, and the region misexpressing the HA-tagged constructs is in green (anti-HA, boundaries outlined in green in *ex-lacZ*-only frames). Details show dorsal hinge regions (middle and right). (**A-E**) In wild-type wing discs, expression of *UAS-ftΔICD* (A), *UAS-ftΔ7-C* (B) or *UAS-ftΔN–5* (D) increases *ex-lacZ* both posterior and just anterior to the boundary of expression. Expression of *ex-lacZ* is approximately equal in posterior and anterior cells after expression of *UAS-ftΔ8-C* (C) or *UAS-ftΔN-4* (E), except along the boundary of *hh-gal4* expression. See supplementary material Fig. S10 for results with additional Ft+ECD constructs. (**F**) *UAS-ftΔICD* increases *ex-lacZ* expression in posterior of *ft* mutant disc; see supplementary material Fig. S12B for a similar experiment with *ban3-GFP*.

ft mutant discs (Fig. 4A; supplementary material Fig. S6B,C, Fig. S7E,F, Fig. S9), but the corresponding Ft+ECD constructs, which lacked the Su(DN) (7-8) domain, rescued more weakly (Fig. 4F; supplementary material Fig. S7K,L, Fig. S13B,C). That said, the levels and pattern of expression probably affect the extent of any dominant-negative effect of the ECD, as the results with *actin-gal4*-driven rescue of eclosion differed slightly (Fig. 1). It is also likely that there is additional complexity in the 6-9 region; despite the similar expression levels of the constructs, rescue of reporter expression and overgrowth with FtΔ8-C was also weak (supplementary material Fig. S7J, Fig. S13A), and rescue of

overgrowth and *ex-lacZ* (although not eclosion) with FtΔ6-C was slightly stronger than with FtΔ7-C (supplementary material Fig. S5, Fig. S7K,L, Fig. S9, Fig. S13B,C).

The ECD of Ft can induce boundary-specific dominant-negative effects

Those Ft+ECD constructs that did not induce *ex-lacZ* expression throughout the posterior of *hh-gal4* discs also had dominant-negative effects, but this effect on *ex-lacZ* was now limited to the boundary of misexpression (Fig. 5C,E; supplementary material Fig. S10A,G-I). In fact, posterior *hh-gal4*-driven overexpression of full-length Ft caused a similar boundary-specific increase in *ex-lacZ* or *ban3-GFP* expression, especially in the prospective hinge regions of the wing disc (Fig. 6A, Fig. 7E). In other words, a gain in Ft expression can cause a boundary-specific loss-of-function phenotype (see also Zecca and Struhl, 2010). The region with heightened *ex-lacZ* expression was wider on the anterior, wild-type side of the boundary, but in most cases also slightly overlapped the posterior.

Such boundary effects do not appear to be caused by apposition of cells with different levels of Hippo pathway activity. *ft* or *warts* mutant clones reduce Hippo pathway activity, but do not induce boundary effects in adjacent wild-type cells (supplementary material Fig. S4A,B). Conversely, posterior expression of FtΔECD in wild-type discs did not cause boundary effects (Fig. 6B). The latter result indicates that the boundary effect requires, and is likely to be mediated by, the ECD of Ft.

Consistent with this hypothesis, the strength of the boundary effect is apparently modulated by the strength Ft-Ds binding. The boundary effect is strongest in the hinge, the region with the highest level of Ds expression. Ft-Ds binding is thought to be reduced further in distal cells by the distal expression of Fj (Brittle et al., 2010; Simon et al., 2010). The boundary effect induced by Ft overexpression extended more distally into the wing pouch when distal *fj* expression was removed (Fig. 6C,D).

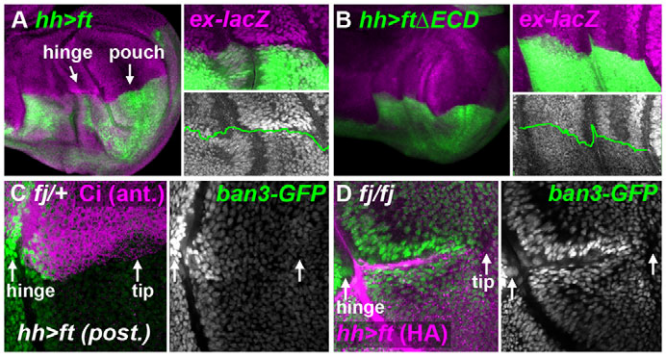

Fig. 6. Induction of boundary effects by the ECD of Ft. Reaction of *ex-lacZ* (purple or white in A,B) or *ban3-GFP* (green or white in C,D) to posterior, *hh-gal4*-driven expression of *UAS-ft* (A,C,D) or *UAS-ftΔECD* (B) in wild-type (A,B), fj^{d1}/+ (C) or fj^{d1}/fj^{d1} (D) wing discs. The posterior region expressing the HA-tagged constructs was marked with anti-HA in A,B (green, boundaries outlined in green) and D (purple), and in C the complementary anterior region was marked with anti-Ci (purple). (**A**,**B**) Posterior *ft* expression upregulates *ex-lacZ* in the hinge region of wild-type discs (A), whereas *ftΔECD* expression does not (B). (**C**,**D**) The upregulation of *ban3-GFP* by posterior *ft* expression was largely limited to the hinge region of *fj*/+ discs (C), but extended further towards the distal tip of the wing pouch in homozygous *fj* discs (D).

The ICD of Ds contributes to dominant-negative effects on the Hippo pathway

The Ft-overexpression boundary effect is reminiscent of similar boundary effects induced by the ECD of Ds; Yki targets are upregulated at the boundary between cells expressing different levels Ds or DsΔICD (Rogulja et al., 2008; Willecke et al., 2008). This response occurs on both sides of the boundary, indicating 'forward' signaling from the overexpressing to wild-type cells and 'reverse' signaling from the wild-type to the overexpressing cells (Fig. 7A,C). Both responses require the presence of *ft*, but Ds also plays a role, not just in initiating these signals, but also in the response to the boundary. If Ds is overexpressed in *ds* mutant discs, it cannot induce a forward dominant-negative response in the adjacent cells that lack *ds*, although the reverse signaling from *ds* mutant cells to the Ds-overexpressing cells is intact (Fig. 7B) (Willecke et al., 2008). If instead DsΔICD is overexpressed in *ds* mutants, not only is the forward signaling lost, but the reverse signal is absent (Willecke et al., 2008), although, in our hands, we detected some reverse signaling in a few rare cases (Fig. 7D). These results suggest that Ds acts, not only as a forward signal that acts via Ft, but also during the reception or transduction of the reverse signal, an activity that is impaired by the loss of the Ds ICD.

We therefore tested whether Ds and Ft are required for the boundary effects induced by Ft overexpression. *hh-gal4*-driven overexpression of Ft induced boundary-specific increases in *ban3-GFP* expression in the hinge regions of wild-type wing discs, but not in *ds* or *ft* mutant wing discs (Fig. 7E,F; data not shown). Similar effects have been noted on *vestigial* quadrant enhancer expression (Zecca and Struhl, 2010).

The dominant-negative effects induced throughout regions of FtΔICD expression were also weakened, although not completely eliminated, by removal of Ds; the proportion of the wing disc occupied by overgrown FtΔICD-expressing cells was much smaller in *ds* mutants and the increase in posterior *ban3-GFP* expression was not as strong (Fig. 7L,M). The negative activity of FtΔICD that remains in *ds* mutants is likely to be mediated by binding to endogenous Ft; FtΔICD stabilizes not only Ds but also endogenous Ft at the cell membrane (Matakatsu and Blair, 2006), and we have not detected dominant-negative effects of FtΔICD on *ban3-GFP* in *ds ft* mutant discs (supplementary material Fig. S12C).

These results suggest that, under some circumstances, Ds and Ft can be converted to forms or locations that inhibit Hippo pathway activity. To investigate further whether an inhibitory Ds activity can be mediated by its ICD, we examined the effects of *hh-gal4*-driven expression of DsΔECD in wild-type and *ds* mutant discs. We could not detect any effect on *ban3-GFP* in wild-type discs, although we could weakly disrupt crossvein spacing and wing shape by *hh-* or *en-gal4*-driven expression of DsΔECD (Matakatsu and Blair, 2006). However, in *ds* mutant discs, DsΔECD induced cell-autonomous increases in *ban3-GFP* expression in the proximal wing hinge (compare the sharp expression change in cells adjacent to the boundary in Fig. 7G with the much weaker effect in cells adjacent to the boundary in the *ds* control shown in 7H), as well as overgrowth of the posterior compartment in wing imaginal discs and adult wings (Fig. 7G,I). We observed a similar effect on *ban3-GFP* in *ft* mutant discs (Fig. 7J; *ft* control shown in 7K). Thus, not only are Ds and its ICD necessary for some dominant-negative effects, but the Ds ICD is sufficient to induce a dominant-negative effect in mutant backgrounds.

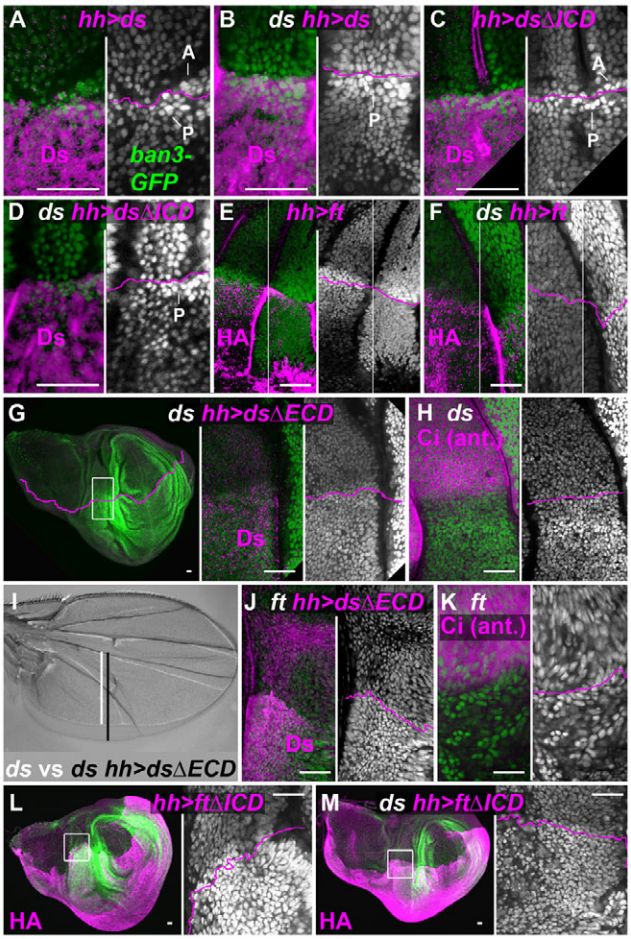

Fig. 7. Role of Ds in mediating the dominant-negative effects of the ECD of Ft. Details show the dorsal hinge region. (**A-D**) Reaction of *ban3-GFP* expression (green, white) in the dorsal hinge region to *hh-gal4*-driven misexpression of *UAS-ds* (A,B) or *UAS-dsΔICD* (C,D) (anti-Ds, purple) in wild-type (A,C) or *ds* mutant (B,D) discs. After *ds* (A) or *dsΔICD* (C) expression in wild type, *ban3-GFP* expression is heightened on both sides of the boundary (purple line; A, anterior; P, posterior). After *ds* expression in *ds* mutants (B), heightened *ban3-GFP* expression is limited to the *ds*-overexpressing side of the boundary. After *dsΔICD* in *ds* mutants, the heightened boundary expression of *ban3-GFP* is very faint, and limited to the misexpressing side (D). (**E**,**F**) Reaction of *ban3-GFP* (green, white) to *UAS-ft* (anti-HA, purple) in wild-type (E) or *ds* mutant (F) wing discs. The Ft overexpression boundaries heightened expression of *ban3-GFP* in wild-type discs (E) but not *ds* mutant discs (F). Right and left halves of each *ban3-GFP* image were taken at a different intensity to avoid saturation of the image by the higher expression in the distal (right) portion of the disc. (**G**) *hh-gal4*-driven expression of *UAS-dsΔECD* (anti-Ds, purple) heightens *ban3-GFP* expression (green, white) in dorsal hinge regions and also induces overgrowth in the posterior compartment in *ds* mutant wing disc. Boxed region is magnified in middle and right panels. (**H**) *ban3-GFP* expression (green, white) in an identical region in the *ds* mutant, with anterior cells marked with anti-Ci (purple). (**I**) Overlay comparing adult wings from *ds* mutant with posterior, *hh-gal4*-driven expression of *UAS-dsΔECD* (gray) to a *ds* mutant control wing (white). White and black bars show the size of the *hh-gal4*-expressing, posterior region in each; DsΔECD induced additional growth in the posterior. (**J**,**K**) *hh-gal4*-driven expression of UAS-*dsΔECD* (anti-Ds, purple) heightens *ban3-GFP* expression (green, white) in the dorsal hinge regions of a *ft* mutant wing disc (J). Control showing *ban3-GFP* expression (green, white) in an identical region in *ft* mutant, with anterior cells marked with anti-Ci (purple) (K). (**L**,**M**) Disc overgrowth and reaction of *ban3-GFP* expression (green or white) after *hh-gal4*-driven expression of *UAS-ftΔICD* (anti-HA, purple) in wild-type (L) or *ds* mutant (M) wing discs. In wild-type discs (L), FtΔICD elevated *ban3-GFP* expression and induced massive overgrowth. In *ds* mutants (M), the elevation of *ban3-GFP* expression was weaker, and FtΔICD domain occupied a smaller proportion of the disc than in wild type (L). Boxed regions are magnified in right panels. Scale bars: 25 μm.

DISCUSSION

Our results first confirm that expression of Ft constructs lacking the ECD, and thus the ability to bind Ds or be phosphorylated by Fj, can improve the overgrowth, Hippo pathway and PCP defects caused by the absence of endogenous Ft, Ds, or both. Second, the ICD domains required for the Hippo signaling and PCP activities of Ft are largely separable, and do not overlap with previously identified protein-binding domains. Finally, we confirm and extend evidence that the ECD of Ft has activities in both the PCP and Hippo pathways that are mediated by Ds, and investigate the role of Ds in the dominant-negative effects on Hippo activity caused by Ft construct overexpression.

A permissive role for unpatterned Ft activity in PCP

The substantial, albeit imperfect, improvement in *ft* mutant PCP defects in wing and abdomens by uniform expression of FtΔECD constructs indicates that the PCP activity of Ft is to some extent permissive, rather than relying purely on the spatial regulation of Ft-Ds binding by gradients or domains of *ds* and *fj* expression. This is also in agreement with the substantial improvement of *ds* and *ds fj* mutant PCP defects by uniformly expressed *ds* and *fj* (Matakatsu and Blair, 2004; Simon, 2004; Aigouy et al., 2010). One hypothesis suggests that the adhesion mediated by uniform Ds provides tension during elongation of the pupal wing blade, aiding in the reorientation of cell polarity along the proximo-distal axis of the wing (Aigouy et al., 2010). But although it is possible that the FtΔECD constructs affect tension in the wing, they cannot do so by binding Ds or other extracellular ligands and thereby mediating cell adhesion.

An alternative is that uniform FtΔECD improves PCP by affecting the Hippo pathway, which can regulate the expression of PCP components like Fj (Feng and Irvine, 2007). However, the improvement of abdominal PCP by FtΔECDΔ1-C, which lacks detectable Hippo pathway activity, argues strongly that the Hippo pathway is not the sole permissive mechanism of Ft PCP activity.

Known protein-binding domains are disposable for Ft ICD function

Our structure-function analyses identified largely distinct regions of the Ft ICD that are active in PCP and Hippo signaling, but their locations are surprising given what is known about the structure of the Ft ICD. The mammalian Ft homolog Fat4 has ICD regions with substantial similarity to the ICD of *Drosophila* Ft (Fig. 1; supplementary material Fig. S1A), but of the regions we identified above, only the PH region, which is weakly active in PCP and Hippo activity, is highly similar to a domain in Fat4; the Hippo N, Hippo C, and PCP regions are not. Nonetheless, these domains have been highly conserved in the 300-350 million years since the divergence of metamorphosing and non-metamorphosing insects (supplementary material Fig. S1B). This probably reflects functional conservation, as the Ft homolog from a non-metamorphosing insect regulates regenerative growth (Bando et al., 2009).

We also found that the known protein-interaction domains in the Ft ICD appear to be disposable. FtΔECDΔ6-C rescues *ft* mutant overgrowth, Hippo pathway and PCP defects, but lacks the binding regions identified for Lowfat, Grunge and Dco (Fig. 1; supplementary material Fig. S1A), and the region most similar to the region of Fat4 sufficient for binding Mpdz. It is unlikely that these regions completely lack function. Indeed, FtΔECDΔ5-6, which lacks Hippo C, had slightly more effect on *ex-lacZ* than did FtΔECDΔ5-C, which also lacks these protein-binding domains (compare supplementary material Fig. S6D and Fig. S8B). We suggest that the 6-C region mediates modulatory interactions that are not absolutely required for the activation of pathways downstream of the Ft ICD. Our method also drives construct expression at higher levels than those of endogenous Ft, and so in this sense assays for the minimal regions required for PCP and Hippo pathway activities.

The presence of distinct PCP and Hippo-active domains is noteworthy, as it indicates that the downstream pathways are largely distinct. The PH domain was the exception, having weak effects on both PCP and the Hippo pathway, leaving open the possibility that increases in Hippo activity pathway might contribute weakly to PCP activity.

Activities of the ECD of Ft and a role for Ds in signal reception

The PCP activity of Ft is not limited to its ICD; deletion constructs containing the ECD did a better job improving *ft* mutant PCP defects than their ΔECD counterparts, and even an Ft construct completely lacking the ICD had weak PCP activity. This latter activity is likely to be due to binding Ds, as it was lost in *ft ds* mutants. A previous report showed that the repolarization of abdominal cells adjacent to cells expressing a different FtΔICD construct (ecto-Ft) was also lost in *ds* mutants (Casal et al., 2006). This strongly suggests that Ft-bound Ds has a weak, redundant role in the reception of PCP signals.

FtΔICD also affects growth and Hippo pathway activity throughout regions of misexpression, but in this case the effect is dominant negative, eliciting overgrowth and suppressing Hippo pathway activity (Fig. 5) (Matakatsu and Blair, 2006; Willecke et al., 2006). Our evidence indicates that this is likely to be mediated by misregulation of the ECD of Ft resulting in non-functional binding to both endogenous Ft and Ds. This misregulation can be elicited by removing several different domains in the Ft ICD. One of these, the Su(DN) domain, overlaps regions sufficient for binding Lowfat and Grunge (Fig. 1), but *lowfat* and *Grunge* mutants have not been reported to cause overgrowth (Fanto et al., 2003; Mao et al., 2009).

However, we found that overexpression of even wild-type Ft caused dominant-negative suppression of Hippo pathway activity that was limited to cells at the boundary of overexpression, and that this effect required the presence of Ds in adjacent cells. Similar effects were also reported during the regulation of *vestigial* quadrant enhancer expression between wing and non-wing portions of wing discs (Zecca and Struhl, 2010). This again suggests a role for Ds in reception, in this case of a dominant-negative signal. This effect is likely to be mediated by the ICD of Ds: we found that overexpression of a form of Ds lacking its ECD can cause suppress Hippo pathway activity in discs sensitized by the removal of endogenous Ft or Ds.

This inhibitory role for Ds is surprising; loss of *ds* slightly increases growth and weakly reduces Hippo pathway activity, showing that Ds has a net positive activity (Matakatsu and Blair, 2006; Rogulja et al., 2008). Although some of the positive activity of Ds might be mediated by binding Ft and increasing Ft activity, removal of endogenous *ds* increases overgrowth in *ft* mutants, indicating that Ds can stimulate Hippo activity independently of Ft (Matakatsu and Blair, 2006). Thus, Ds can either stimulate or inhibit Hippo pathway activity depending on the context; indeed, the stronger dominant-negative effects of DsΔECD in *ds* mutants suggest that in wild-type discs it is competing with the positive activity of endogenous Ds.

Modeling the effects of boundaries of Ft-Ds binding

The dominant-negative effects at Ft overexpression boundaries are similar to the effects previously reported at boundaries of Ds or DsΔICD misexpression (Rogulja et al., 2008; Willecke et al., 2008). The hypothesis that Ft and Ds both send and receive signals provides an attractive explanation for these effects. Signal reception by Ds accounts for the 'forward', Ds-dependent signaling from Ft-overexpressing cells to adjacent cells. It also could explain the 'backward' signaling from adjacent cells back to regions of Ds overexpression. Because this reverse signaling is not blocked by removing Ds from the adjacent cells, it is likely to be initiated by the Ft expressed in those cells; the reverse signal depends in part on having full-length Ds in the receiving cells (Fig. 7A-D) (Willecke et al., 2008).

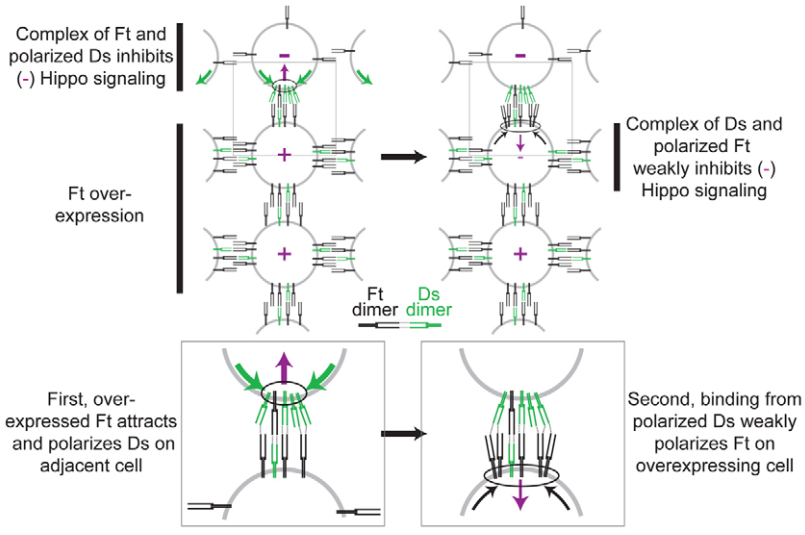

Fig. 8. Model for the inhibition of Hippo signaling at boundaries of Ft overexpression. Binding between Ft (black) and Ds (green) normally promotes (+) Hippo signaling via the ICD of Ft. The heightened expression of Ft in posterior cells first recruits and polarizes the Ds dimers on anterior cells to the adjacent cell face, creating a Ds-Ft complex (circled) that inhibits (–) Hippo signaling. Next, unoccupied binding sites on the polarized Ds dimers weakly recruit and polarize Ft on posterior cells, creating a Ds-Ft complex that weakly inhibits Hippo signaling.

But why does overexpression of Ft, Ds or DsΔICD inhibit Hippo pathway in boundary cells, without causing a similar effect throughout the region of misexpression? One boundary-specific activity that has been invoked is the 'capping' or polarized redistribution of binding partners on the surface of a cell (Reddy and Irvine, 2008; Rogulja et al., 2008). Ft or Ds is attracted to the face of the cell that neighbors another cell expressing its binding partner at high levels, and is depleted from the other faces of the cell (Strutt and Strutt, 2002; Ma et al., 2003; Matakatsu and Blair, 2004). Moreover, if the capped binding partners had vacant binding domains (or recruited cis homodimers that had vacant binding sites), this might result in concentrated 'reverse' binding to the neighboring face of the overexpressing cell (Fig. 8). For instance, Ft overexpression could induce localized binding and concentration of Ds on the neighboring face of an adjacent wild-type cell, and the concentrated Ds would heighten the levels of Ds-bound Ft in the neighboring face of the Ft-overexpressing cell. The reverse effect would probably be weaker, explaining the weaker reverse signaling we observe at Ft-overexpression boundaries.

It has been suggested that the Ds-driven polarization of Ft inhibits Hippo pathway activity because it depletes Ft from the other faces of the cell, creating an *ft*-mutant-like situation on the depleted cell faces and, thereby, a mutant-like phenotype (Reddy and Irvine, 2008; Rogulja et al., 2008). However, this explanation is less satisfying for signaling at boundaries of Ft overexpression, because the depletion of Ds from non-adjacent cell faces cannot on its own be the cause of the boundary effect. Complete loss of Ds causes only very slight overgrowth (Matakatsu and Blair, 2006) and subtle upregulation of Yki targets (Rogulja et al., 2008), whereas our boundary effects on these markers resemble the much stronger changes observed in *ft* mutant clones. We therefore prefer the hypothesis that when Ft and Ds are clustered on one face of the polarized cell they not only lose their ability to increase Hippo activity, but are converted to a form or location that inhibits Hippo activity, for instance by forming a complex that sequesters Hippo pathway components on their ICDs (Fig. 8).

Acknowledgements
We thank Dr Miho Tanaka-Matakatsu for the *bantam* regulatory DNA.

Funding
This work was supported by grants from the National Institutes of Health [R01-NS028202] and the National Science Foundation [IOS-0818539]. Deposited in PMC for release after 12 months.

Competing interests statement
The authors declare no competing financial interests.

Supplementary material
Supplementary material available online at
http://dev.biologists.org/lookup/suppl/doi:10.1242/dev.070367/-/DC1

References

Adler, P. N., Charlton, J. and Liu, J. (1998). Mutations in the cadherin superfamily member gene *dachsous* cause a tissue polarity phenotype by altering frizzled signaling. *Development* **125**, 959-968.
Aigouy, B., Farhadifar, R., Staple, D. B., Sagner, A., Roper, J. C., Julicher, F. and Eaton, S. (2010). Cell flow reorients the axis of planar polarity in the wing epithelium of *Drosophila*. *Cell* **142**, 773-786.
Bando, T., Mito, T., Maeda, Y., Nakamura, T., Ito, F., Watanabe, T., Ohuchi, H. and Noji, S. (2009). Regulation of leg size and shape by the Dachsous/Fat signalling pathway during regeneration. *Development* **136**, 2235-2245.
Barolo, S., Carver, L. A. and Posakony, J. W. (2000). GFP and galactosidase transformation vectors for promoter/enhancer analysis in *Drosophila*. *Biotechniques* **29**, 726-732.
Bennett, F. C. and Harvey, K. F. (2006). Fat cadherin modulates organ size in *Drosophila* via the Salvador/Warts/Hippo signaling pathway. *Curr. Biol.* **16**, 2101-2110.
Blair, S. S. (2000). Imaginal discs. In *Drosophila Protocols* (ed. W. Sullivan, M. Ashburner and R. S. Hawley), pp. 159-173. Cold Spring Harbor, N.Y.: Cold Spring Harbor Laboratory Press.
Boedigheimer, M. and Laughon, A. (1993). Expanded: a gene involved in the control of cell proliferation in imaginal discs. *Development* **118**, 1291-1301.
Brittle, A. L., Repiso, A., Casal, J., Lawrence, P. A. and Strutt, D. (2010). Four-jointed modulates growth and planar polarity by reducing the affinity of dachsous for fat. *Curr. Biol.* **20**, 803-810.
Bryant, P. J., Huettner, B., Held, L. I., Jr, Ryerse, J. and Szidonya, J. (1988). Mutations at the fat locus interfere with cell proliferation control and epithelial morphogenesis in *Drosophila*. *Dev. Biol.* **129**, 541-554.
Buratovich, M. A. and Bryant, P. J. (1997). Enhancement of overgrowth by gene interactions in lethal(2)giant discs imaginal discs from *Drosophila melanogaster*. *Genetics* **147**, 657-670.
Casal, J., Struhl, G. and Lawrence, P. A. (2002). Developmental compartments and planar polarity in *Drosophila*. *Curr. Biol.* **12**, 1189-1198.
Casal, J., Lawrence, P. A. and Struhl, G. (2006). Two separate molecular systems, Dachsous/Fat and Starry night/Frizzled, act independently to confer planar cell polarity. *Development* **133**, 4561-4572.
Cho, E., Feng, Y., Rauskolb, C., Maitra, S., Fehon, R. and Irvine, K. D. (2006). Delineation of a Fat tumor suppressor pathway. *Nat. Genet.* **38**, 1142-1150.
Clark, H. F., Brentrup, D., Schneitz, K., Bieber, A., Goodman, C. and Noll, M. (1995). Dachsous encodes a member of the cadherin superfamily that controls imaginal disc morphogenesis in *Drosophila*. *Genes Dev.* **9**, 1530-1542.
Djiane, A., Yogev, S. and Mlodzik, M. (2005). The apical determinants aPKC and dPatj regulate Frizzled-dependent planar cell polarity in the *Drosophila* eye. *Cell* **121**, 621-631.
Donoughe, S. and DiNardo, S. (2011). dachsous and frizzled contribute separately to planar polarity in the *Drosophila* ventral epidermis. *Development* **138**, 2751-2759.
Fanto, M., Clayton, L., Meredith, J., Hardiman, K., Charroux, B., Kerridge, S. and McNeill, H. (2003). The tumor-suppressor and cell adhesion molecule Fat controls planar polarity via physical interactions with Atrophin, a transcriptional co-repressor. *Development* **130**, 763-774.
Feng, Y. and Irvine, K. D. (2007). Fat and Expanded act in parallel to regulate growth through Warts. *Proc. Natl. Acad. Sci. USA* **104**, 20362-20367.
Feng, Y. and Irvine, K. D. (2009). Processing and phosphorylation of the Fat receptor. *Proc. Natl. Acad. Sci. USA* **106**, 11989-11994.
Garoia, F., Guerra, D., Pezzoli, M. C., Lopez-Varea, A., Cavicchi, S. and Garcia-Bellido, A. (2000). Cell behaviour of *Drosophila* fat cadherin mutations in wing development. *Mech. Dev.* **94**, 95-109.
Hogan, J., Valentine, M., Cox, C., Doyle, K. and Collier, S. (2011). Two frizzled planar cell polarity signals in the *Drosophila* wing are differentially organized by the Fat/Dachsous pathway. *PLoS Genet.* **7**, e1001305.
Hong, J. C., Ivanov, N. V., Hodor, P., Xia, M., Wei, N., Blevins, R., Gerhold, D., Borodovsky, M. and Liu, Y. (2004). Identification of new human cadherin genes using a combination of protein motif search and gene finding methods. *J. Mol. Biol.* **337**, 307-317.
Ishikawa, H. O., Takeuchi, H., Haltiwanger, R. S. and Irvine, K. D. (2008). Four-jointed is a Golgi kinase that phosphorylates a subset of cadherin domains. *Science* **321**, 401-404.
Ishiuchi, T., Misaki, K., Yonemura, S., Takeichi, M. and Tanoue, T. (2009). Mammalian Fat and Dachsous cadherins regulate apical membrane organization in the embryonic cerebral cortex. *J. Cell Biol.* **185**, 959-967.
Lee, T., Hacohen, N., Krasnow, M. and Montell, D. J. (1996). Regulated Breathless receptor tyrosine kinase activity required to pattern cell migration and branching in the *Drosophila* tracheal system. *Genes Dev.* **10**, 2912-2921.
Ma, D., Yang, C. H., McNeill, H., Simon, M. A. and Axelrod, J. D. (2003). Fidelity in planar cell polarity signalling. *Nature* **421**, 543-547.
Mao, Y., Rauskolb, C., Cho, E., Hu, W. L., Hayter, H., Minihan, G., Katz, F. N. and Irvine, K. D. (2006). Dachs: an unconventional myosin that functions downstream of Fat to regulate growth, affinity and gene expression in *Drosophila*. *Development* **133**, 2539-2551.
Mao, Y., Kucuk, B. and Irvine, K. D. (2009). *Drosophila* lowfat, a novel modulator of Fat signaling. *Development* **136**, 3223-3233.
Mao, Y., Mulvaney, J., Zakaria, S., Yu, T., Morgan, K. M., Allen, S., Basson, M. A., Francis-West, P. and Irvine, K. D. (2011). Characterization of a Dchs1 mutant mouse reveals requirements for Dchs1-Fat4 signaling during mammalian development. *Development* **138**, 947-957.
Matakatsu, H. and Blair, S. S. (2004). Interactions between Fat and Dachsous and the regulation of planar cell polarity in the *Drosophila* wing. *Development* **131**, 3785-3794.
Matakatsu, H. and Blair, S. S. (2006). Separating the adhesive and signaling functions of the Fat and Dachsous protocadherins. *Development* **133**, 2315-2324.
Matakatsu, H. and Blair, S. S. (2008). The DHHC palmitoyltransferase approximated regulates Fat signaling and Dachs localization and activity. *Curr. Biol.* **18**, 1390-1395.

Motzny, C. K. and Holmgren, R. (1995). The *Drosophila* cubitus interruptus protein and its role in the wingless and hedgehog signal transduction pathways. *Mech. Dev.* **52**, 137-150.
Nolo, R., Morrison, C. M., Tao, C., Zhang, X. and Halder, G. (2006). The bantam microRNA is a target of the hippo tumor-suppressor pathway. *Curr. Biol.* **16**, 1895-1904.
Oh, H. and Irvine, K. D. (2008). In vivo regulation of Yorkie phosphorylation and localization. *Development* **135**, 1081-1088.
Pan, D. (2010). The hippo signaling pathway in development and cancer. *Dev. Cell* **19**, 491-505.
Qi, C., Zhu, Y. T., Hu, L. and Zhu, Y. J. (2009). Identification of Fat4 as a candidate tumor suppressor gene in breast cancers. *Int. J. Cancer* **124**, 793-798.
Queenan, A. M., Ghabrial, A. and Schupbach, T. (1997). Ectopic activation of torpedo/Egfr, a *Drosophila* receptor tyrosine kinase, dorsalizes both the eggshell and the embryo. *Development* **124**, 3871-3880.
Rawls, A. S., Guinto, J. B. and Wolff, T. (2002). The cadherins fat and dachsous regulate dorsal/ventral signaling in the *Drosophila* eye. *Curr. Biol.* **12**, 1021-1026.
Reddy, B. V. and Irvine, K. D. (2008). The Fat and Warts signaling pathways: new insights into their regulation, mechanism and conservation. *Development* **135**, 2827-2838.
Repiso, A., Saavedra, P., Casal, J. and Lawrence, P. A. (2010). Planar cell polarity: the orientation of larval denticles in *Drosophila* appears to depend on gradients of Dachsous and Fat. *Development* **137**, 3411-3415.
Rogulja, D., Rauskolb, C. and Irvine, K. D. (2008). Morphogen control of wing growth through the Fat signaling pathway. *Dev. Cell* **15**, 309-321.
Saburi, S., Hester, I., Fischer, E., Pontoglio, M., Eremina, V., Gessler, M., Quaggin, S. E., Harrison, R., Mount, R. and McNeill, H. (2008). Loss of Fat4 disrupts PCP signaling and oriented cell division and leads to cystic kidney disease. *Nat. Genet.* **40**, 1010-1015.
Saucedo, L. and Edgar, B. (2007). Filling out the Hippo pathway. *Nat. Rev. Mol. Cell Biol.* **8**, 613-621.
Silva, E., Tsatskis, Y., Gardano, L., Tapon, N. and McNeill, H. (2006). The tumor-suppressor gene *fat* controls tissue growth upstream of Expanded in the Hippo signaling pathway. *Curr. Biol.* **16**, 2081-2089.
Simon, M. A. (2004). Planar cell polarity in the *Drosophila* eye is directed by graded Four-jointed and Dachsous expression. *Development* **131**, 6175-6184.
Simon, M. A., Xu, A., Ishikawa, H. O. and Irvine, K. D. (2010). Modulation of Fat:Dachsous binding by the cadherin domain kinase four-jointed. *Curr. Biol.* **20**, 811-817.
Sopko, R., Silva, E., Clayton, L., Gardano, L., Barrios-Rodiles, M., Wrana, J., Varelas, X., Arbouzova, N. I., Shaw, S., Saburi, S. et al. (2009). Phosphorylation of the tumor suppressor fat is regulated by its ligand Dachsous and the kinase discs overgrown. *Curr. Biol.* **19**, 1112-1117.
Strutt, H. and Strutt, D. (2002). Nonautonomous planar polarity patterning in *Drosophila*: dishevelled-independent functions of frizzled. *Dev. Cell* **3**, 851-863.
Tanaka-Matakatsu, M., Xu, J., Cheng, L. and Du, W. (2009). Regulation of apoptosis of rbf mutant cells during *Drosophila* development. *Dev. Biol.* **326**, 347-356.
Thompson, B. J. and Cohen, S. M. (2006). The Hippo pathway regulates the bantam microRNA to control cell proliferation and apoptosis in *Drosophila*. *Cell* **126**, 767-774.
Tyler, D. M. and Baker, N. E. (2007). Expanded and fat regulate growth and differentiation in the *Drosophila* eye through multiple signaling pathways. *Dev. Biol.* **305**, 187-201.
Van Hateren, N. J., Das, R. M., Hautbergue, G. M., Borycki, A. G., Placzek, M. and Wilson, S. A. (2011). FatJ acts via the Hippo mediator Yap1 to restrict the size of neural progenitor cell pools. *Development* **138**, 1893-1902.
Willecke, M., Hamaratoglu, F., Kango-Singh, M., Udan, R., Chen, C. L., Tao, C., Zhang, X. and Halder, G. (2006). The Fat cadherin acts through the Hippo tumor-suppressor pathway to regulate tissue size. *Curr. Biol.* **16**, 2090-2100.
Willecke, M., Hamaratoglu, F., Sansores-Garcia, L., Tao, C. and Halder, G. (2008). Boundaries of Dachsous Cadherin activity modulate the Hippo signaling pathway to induce cell proliferation. *Proc. Natl. Acad. Sci. USA* **105**, 14897-14902.
Yang, C. H., Axelrod, J. D. and Simon, M. A. (2002). Regulation of Frizzled by fat-like cadherins during planar polarity signaling in the *Drosophila* compound eye. *Cell* **108**, 675-688.
Zecca, M. and Struhl, G. (2010). A feed-forward circuit linking wingless, fat-dachsous signaling, and the warts-hippo pathway to *Drosophila* wing growth. *PLoS Biol.* **8**, e1000386.
Zeidler, M. P., Perrimon, N. and Strutt, D. I. (1999). The *four-jointed* gene is required in the *Drosophila* eye for ommatidial polarity specification. *Curr. Biol.* **9**, 1363-1372.
Zeidler, M. P., Perrimon, N. and Strutt, D. I. (2000). Multiple roles for *four-jointed* in planar polarity and limb patterning. *Dev. Biol.* **228**, 181-196.

Table S1. Details of Ft constructs

Construct	Amino acid sequence
FtΔECD	MERLLLLFFLLLAGRESLCQTGDTKLELLAPRGRSYATTYEQYAAFPRR RSSSSSPSGEMQSRAVDTS partial cadherin domain: ADFEVLEGQPRGTTVGFIPTKPKFSYRFNEPPREFTLDPVTGEVKTNVVL DREGMRDHYDLVVLSSQPT^{137}- C^{4569}RGD…EEYV^{5147}-YPYDVPDYA*
FtΔECD2	MERLLLLFFLLLAGRESLCQTGDTKLELLAPRGRSYATT^{39}-C^{4569}RGD…E EYV^{5147}-YPYDVPDYA*
FtICD	M-F^{4611}RGKQ…EEYV^{5147}-YPYDVPDYA*
λFtICD	FGF receptor 1: MVTWRCLILWAVLVTATLSAARPAPTLPDQALPKANIEVESHSAHPGDL LQL- cI dimerization domain: SLRSEYEYPVFSFRGKHVQAGMFSPELRTFTKGDAERWVSTTKKASDS AFWLEVEGNSMTAPTGSKPSFPDGMLILVDPEQAVEPGDFCIARLGGD EFTFKKLIRDSGQVFLQPLNPQYPMIPCNESCSVVGKVIASQWPEETFG- FGF receptor 1: QYTCLAANSIGISHHSAWLTVLKVEDNKPALLASPLQ- Breathless transmembrane: LEIYALLHAHPLGFTLAAITIVALFLLGSAFIT- F^{4611}RGK…EEYV^{5147}-YPYDVPDYA*
ΔN-1	RFRG^{4613}-R^{4701}PQR…EEYV^{5147}-YPYDVPDYA*
ΔN-2	RFRG^{4613}-A^{4734}SSV…EEYV^{5147}-YPYDVPDYA*
ΔN-4	RFRG^{4613}-L^{4775}RKY…EEYV^{5147}-YPYDVPDYA*
ΔN-5	RFRG^{4613}-L^{4835}ARL…EEYV^{5147}-YPYDVPDYA*
ΔN-6	RFRG^{4613}-Q^{4915}AQQ…EEYV^{5147}-YPYDVPDYA*
Δ9-C	GPSQ^{5120}-YPYDVPDYA*

Δ8-C	ASPS^{6083}-YPYDVPDYA*
Δ7-C	PTTV^{5034}-YPYDVPDYA*
Δ6-C	QQTS^{4920}-YPYDVPDYA*
Δ5-C	LARL^{4838}-*
Δ4-C	ASVP^{4783}-YPYDVPDYA*
Δ2-C	PLEH^{4733}-YPYDVPDYA*
Δ1-C	QRPD^{4706}-YPYDVPDYA*
ΔICD	EKIG^{4619}-YPYDVPDYA*
Δ5-6	LARL^{4838}-AAA-M^{4921}GLT…EEYV^{5147}-YPYDVPDYA*
Δ1-3	QQQQ^{4700}-AA-A^{4752}SSI…EEYV^{5147}-YPYDVPDYA*
Δ3-4	LENA^{4752}-AA-L^{4775}RKY…EEYV^{5147}-YPYDVPDYA*
Δ3-5	LENA^{4752}-A-A^{4836}RLS…EEYV^{5147}-YPYDVPDYA*
Δ1-5	QQQQ^{4700}-AA-A^{4836}RLS…EEYV^{5147}-YPYDVPDYA*

-, splice sites; …, Ft sequences that are not shown but are present in the constructs.
HA tags are underlined.
Other construct-specific domains are as indicated.